 CMES, vol.1403, no.1, pp.1-19, 2009

Free Vibration Analysis of a Circular Plate with Multiple Circular Holes by Using the Multipole Trefftz Method

Wei-Ming Lee[1] **and Jeng-Tzong Chen**[2]

Abstract: This paper presents the multipole Trefftz method to derive an analytical model describing the free vibration of a circular plate with multiple circular holes. Based on the addition theorem, the solution of multipoles centered at each circle can be expressed in terms of multipoles centered at one circle, where boundary conditions are specified. In this way, a coupled infinite system of simultaneous linear algebraic equations is derived for the circular plate with multiple holes. The direct searching approach is employed in the truncated finite system to determine the natural frequencies by using singular value decomposition (SVD). After determining the unknown coefficients of the multipole representation for the displacement field, the corresponding natural modes are determined. Some numerical eigensolutions are presented and further utilized to explain some physical phenomenon such as the dynamic stress concentration. No spurious eigensolutions can be found in the proposed formulation. Excellent accuracy, fast rate of convergence and high computational efficiency are the main features of the present method thanks to the analytical procedure.

Keywords: free vibration, plate, the multipole Trefftz method, addition theorem, SVD

1 Introduction

Circular plates with multiple circular holes are widely used in engineering structures [Khurasia and Rawtani (1978)], e.g. missiles, aircraft, etc., either to reduce the structure weight or to increase the range of inspection. In addition, the rotating machinery such as disk brake system, circular saw blades, and hard disk for data storage is the practical application for the title problem [Tseng and Wickert (1994)].

---

[1] Department of Mechanical Engineering, China University of Science and Technology, Taipei, Taiwan

[2] Department of Harbor and River Engineering, National Taiwan Ocean University, Keelung, Taiwan. Corresponding author. jtchen@mail.ntou.edu.tw

These holes in the structure usually cause the change of natural frequency as well as the decrease of load carrying capacity. It is important to comprehend the associated effects on the work of mechanical design or the associated controller design. As quoted by Leissa [Leissa and Narita (1980)]: "the free vibrations of circular plates have been of practical and academic interest for at least a century and a half", we revisit this problem by proposing an analytical approach in this paper.

Over the past few decades, most of the researches have focused on the analytical solutions for natural frequencies of the circular or annular plates [Vogel and Skinner (1965); Vera, Sanchez, Laura and Vega (1998); Vega, Vera, Sanchez, and Laura (1998); Vera, Laura and Vega (1999)]. Recently, some researchers intended to extend an annular plate to a circular plate with an eccentric hole. Cheng *et al.* [Cheng, Li, and Yam (2003)] encountered difficulty and resorted to finite element method to implement the vibration analysis of annular-like plates due to the complicated expression for this kind of plate. Laura *et al.* [Laura, Masia, and Avalos (2006)] determined the natural frequencies of circular plate with an eccentric hole by using the Rayleigh-Ritz variational method where the assumed function does not satisfy the natural boundary condition in the inner free edge. Lee *et al.* [Lee, Chen and Lee (2007); Lee and Chen (2008a)] proposed a semi-analytical approach to the free vibration analysis of a circular plate with multiple holes by using the indirect boundary integral method and the null field integral equation method, respectively. They pointed out that some results of Laura [Laura, Masia, and Avalos (2006)] are not accurate enough after careful comparisons. However spurious eigenvalues occur even though the complex-valued kernel function is employed, when the boundary method (BEM) or the boundary integral equation method (BIEM) is used to solve the eigenproblem [Lee and Chen (2008a)]. It is well known that spurious and fictitious frequencies stem from the non uniqueness of solution. Specifically, spurious eigenvalues arise from the incomplete solution representation such as the real-part BEM, multiple reciprocity method. Therefore how to construct the complete solution representation and to keep spurious eigenvalue away is our concern.

The Trefftz method was first presented by Trefftz in 1926 [Trefftz (1926)]. On the boundary alone, this method proposed to construct the solution space using trial complete functions which satisfy the given differential equation [Kamiya and Kita (1995)]. Just as BEM, BIEM or the method of fundamental solution [Reutskiy (2005); Alves and Antunes (2005); Chen, Fan, Young, Murugesan and Tsai (2005); Reutskiy (2006); Reutskiy (2007)], Trefftz method is also categorized as the boundary-type method which can reduce the dimension of the original problem by one. Consequently the number of the unknowns is much less than that of the domain type methods such as finite difference method (FDM) or finite element method (FEM). Moreover the Trefftz formulation is regular and free of the problem of improper boundary integrals. However, almost all the problems solved by using Trefftz method are limited to the simply-connected domain. The extension to problems with holes, i.e. multiply-connected domain, is our concern in this paper.

The concept of multipole method to solve multiply-connected domain problems was firstly devised by Záviška [Záviška (1913)] and used for the interaction of waves with arrays of circular cylinders by Linton and Evans [Linton and Evans (1990)]. Recently, one monograph by Martin [Martin (2006)] used these and other methods to solve problems of the multiple scattering in acoustics, electromagnetism, seismology and hydrodynamics. However, the biHelmholtz interior problem with the fourth order differential equation was not mentioned therein.

This paper proposed the multipole Trefftz method to solve plate problems with the multiply-connected domain in an analytical way. When considering a circular plate with multiple circular holes, the transverse displacement field is expressed as an infinite sum of multipoles at the center of each circle, including an outer circular plate and several inner holes. By using the addition theorem, it is transformed into the same coordinate centered at the corresponding circle, where the boundary conditions are specified. According to the specified boundary conditions, a coupled infinite system of simultaneous linear algebraic equations is obtained. Based on the direct searching approach [Kitahara (1985)], the nontrivial eigensolution can be determined by finding the zero determinant of the truncated finite system through the technique of singular value decomposition (SVD). After determining the unknown coefficients, the corresponding natural modes can be obtained. Several numerical examples are presented and the proposed results of a circular plate with one or three circular holes are compared with those of the semi-analytical solutions [Lee and Chen (2008a)] and the FEM using the ABAQUS. Since BIEM or BEM results in spurious eigenvalues for problems with holes, the appearance of spurious solution by using the present method will be examined here. In addition, the results of eigensolution for the plate with two holes can be used to account for the dynamic stress concentration which occurs in the area between two holes when they are close to each other.

2 Problem statement of plate eigenproblem

A uniform thin circular plate with H circular holes centered at the position vector O_k ($k = 0, 1, \ldots, H$ and O_0 is the position vector of the center of the outer circular plate) has a domain Ω which is enclosed with boundary

$$B = \bigcup_{k=0}^{H} B_k, \tag{1}$$

as shown in Figure 1, where R_k denotes the radius of the kth circle. The governing equation of the free flexural vibration for this plate is expressed as:

$$\nabla^4 w(x) = \lambda^4 w(x), \qquad x \in \Omega, \tag{2}$$

where ∇^4 is the biharmonic operator, w is the lateral displacement, $\lambda^4 = \omega^2 \rho_0 h/D$, λ is the dimensionless frequency parameter, ω is the circular frequency, ρ_0 is the volume density, h is the plate thickness, $\mathrm{D} = \mathrm{Eh}^3/12(1-\mu^2)$ is the flexural rigidity of the plate, E denotes the Young's modulus and μ is the Poisson's ratio.

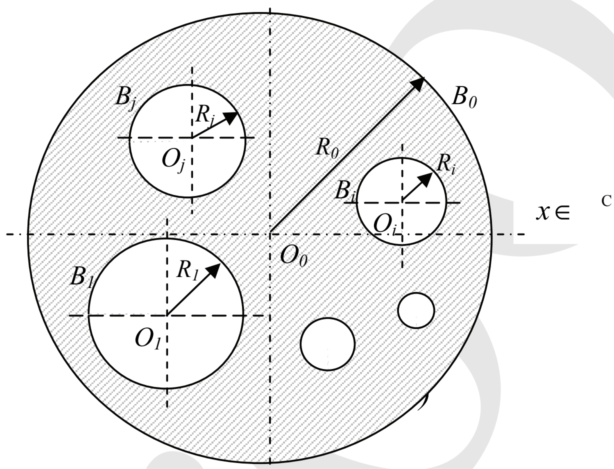

Figure 1: Problem statement for an eigenproblem of a circular plate with multiple circular holes

The solution of Eq. (2) in the polar coordinate can be represented as

$$w(\rho,\varphi) = w_1(\rho,\varphi) + w_2(\rho,\varphi), \tag{3}$$

where $w_1(\rho,\varphi)$ and $w_2(\rho,\varphi)$ are solutions of the following equations, respectively,

$$\nabla^2 w_1(\rho,\varphi) + \lambda^2 w_1(\rho,\varphi) = 0, \tag{4}$$

$$\nabla^2 w_2(\rho,\varphi) - \lambda^2 w_2(\rho,\varphi) = 0. \tag{5}$$

Eqs. (4) and (5) are the so-called Helmholtz equation and the modified Helmholtz equation, respectively. From solutions of Eqs. (4) and (5), the solution for Eq.(3) can be explicitly expressed in series form as follows:

$$w(\rho,\phi) = \sum_{m=-\infty}^{\infty} \tilde{w}_m(\rho) e^{im\phi}, \tag{6}$$

where $\tilde{w}_m(\rho)$ is defined by

$$\tilde{w}_m(\rho) = c_1 J_m(\lambda\rho) + c_2 Y_m(\lambda\rho) + c_3 I_m(\lambda\rho) + c_4 K_m(\lambda\rho), \tag{7}$$

in which c_i ($i = 1, 4$) are the coefficients, J_m andY_m are the mth order Bessel functions; and I_m and K_m are the mth order modified Bessel functions. Based on the characteristics of functions at r=0 and $r \to \infty$, the appropriate Bessel function and the modified Bessel are chosen to represent the transverse displacement field for the outer circular plate and the inner circular holes.

The radial slope, bending moment and effective shear force are related to the transverse displacement by

$$\theta(\rho,\phi) = \frac{\partial w(\rho,\phi)}{\partial\rho}, \tag{8}$$

$$m(\rho,\phi) = \mu\nabla^2 w(\rho,\phi) + (1-\mu)\frac{\partial^2 w(\rho,\phi)}{\partial\rho^2}, \tag{9}$$

$$v(\rho,\varphi) = \frac{\partial}{\partial\rho}\left(\nabla^2 w(\rho,\varphi)\right) + (1-\mu)\left(\frac{1}{\rho}\right)\frac{\partial}{\partial\varphi}\left[\frac{\partial}{\partial\rho}\left(\frac{1}{\rho}\frac{\partial w(\rho,\varphi)}{\partial\varphi}\right)\right]. \tag{10}$$

3 Analytical derivations for the eigensolutions of a circular plate with multiple circular holes

Considering a circular plate with H circular holes, the lateral displacement of Eq. (3) can be explicitly expressed as an infinite sum of multipoles at the center of each circle,

$$\begin{aligned} w(x;\rho_0,\phi_0,\rho_1,\phi_1,\ldots,\rho_H,\phi_H) = & \sum_{m=-\infty}^{\infty}\left(a_m^0 J_m(\lambda\rho_0)e^{im\phi_0} + b_m^0 I_m(\lambda\rho_0)e^{im\phi_0}\right) \\ & + \sum_{k=1}^{H}\left[\sum_{m=-\infty}^{\infty} a_m^k H_m^{(1)}(\lambda\rho_k)e^{im\phi_k} + b_m^k K_m(\lambda\rho_k)e^{im\phi_k}\right], \end{aligned} \tag{11}$$

where (ρ_0,φ_0), (ρ_0,φ_0), $\ldots$, (ρ_H,φ_H) are the corresponding polar coordinates for the field point $\boldsymbol{x}$ with respect to each center of circle. The coefficients of a_m^k and b_m^k, k=0,..., H; m=0, ± 1, ± 2, ...can be determined by applying the boundary condition on each circle. The Bessel function J and the modified Bessel function I are chosen to represent the outer circular plate due to the request of finite value at r=0. For the inner holes, the Hankel function (J+iY) and the modified Bessel function K are taken for their values being finite as $r \to \infty$.

Based on the Graf's addition theorem for the Bessel functions given in [Watson (1995)], we can express the theorem in the following form,

$$J_m(\lambda\rho_k)\mathrm{e}^{im\phi_k} = \sum_{n=-\infty}^{\infty} J_{m-n}(\lambda r_{kp})\mathrm{e}^{i(m-n)\theta_{kp}} J_n(\lambda\rho_p)e^{in\phi_p}, \tag{12}$$

$$I_m(\lambda\rho_k)\mathrm{e}^{im\phi_k} = \sum_{n=-\infty}^{\infty} I_{m-n}(\lambda r_{kp})\mathrm{e}^{i(m-n)\theta_{kp}} I_n(\lambda\rho_p)e^{in\phi_p}, \tag{13}$$

$$H_m^{(1)}(\lambda\rho_k)\mathrm{e}^{im\varphi_k} = \begin{cases} \sum\limits_{n=-\infty}^{\infty} H_{m-n}^{(1)}(\lambda r_{kp})\mathrm{e}^{i(m-n)\theta_{kp}} J_n(\lambda\rho_p)e^{in\varphi_p}, \rho_p < r_{kp} \\ \sum\limits_{n=-\infty}^{\infty} J_{m-n}(\lambda r_{kp})\mathrm{e}^{i(m-n)\theta_{kp}} H_n^{(1)}(\lambda\rho_p)e^{in\varphi_p}, \rho_p > r_{kp} \end{cases}, \tag{14}$$

$$K_m(\lambda\rho_k)\mathrm{e}^{im\varphi_k} = \begin{cases} \sum\limits_{n=-\infty}^{\infty} (-1)^n K_{m-n}(\lambda r_{kp})\mathrm{e}^{i(m-n)\theta_{kp}} I_n(\lambda\rho_p)e^{in\varphi_p}, & \rho_p < r_{kp} \\ \sum\limits_{n=-\infty}^{\infty} (-1)^{m-n} I_{m-n}(\lambda r_{kp})\mathrm{e}^{i(m-n)\theta_{kp}} K_n(\lambda\rho_p)e^{in\varphi_p}, & \rho_p > r_{kp} \end{cases}, \tag{15}$$

where (ρ_p, ϕ_p) and (ρ_k, φ_k) in Fig. 2 are the polar coordinates of a field point $\boldsymbol{x}$ with respect to O_p and O_k, respectively, which are the origins of two polar coordinate systems and (r_{pk}, θ_{pk}) are the polar coordinates of O_k with respect to O_p.

By substituting the addition theorem of the Bessel functions $H_m^{(1)}(\lambda\rho_k)$ and $K_m(\lambda\rho_k)$into Eq. (11), the displacement field near the circular boundary B_0 under the condition of $\rho_0 > r_{k0}$ can be expanded as follows:

$$\begin{aligned} w(x;\rho_0,\phi_0) = &\sum_{m=-\infty}^{\infty} \left(a_m^0 J_m(\lambda\rho_0)e^{im\phi_0} + b_m^0 I_m(\lambda\rho_0)e^{im\phi_0}\right) \\ &+ \sum_{k=1}^{H}\left[\sum_{m=-\infty}^{\infty} a_m^k \sum_{n=-\infty}^{\infty} J_{m-n}(\lambda r_{k0})\mathrm{e}^{i(m-n)\theta_{k0}} H_n^{(1)}(\lambda\rho_0)e^{in\phi_0}\right. \\ &\left. + b_m^k \sum_{n=-\infty}^{\infty} (-1)^{m-n} I_{m-n}(\lambda r_{k0})\mathrm{e}^{i(m-n)\theta_{k0}} K_n(\lambda\rho_0)e^{in\phi_0}\right]. \end{aligned} \tag{16}$$

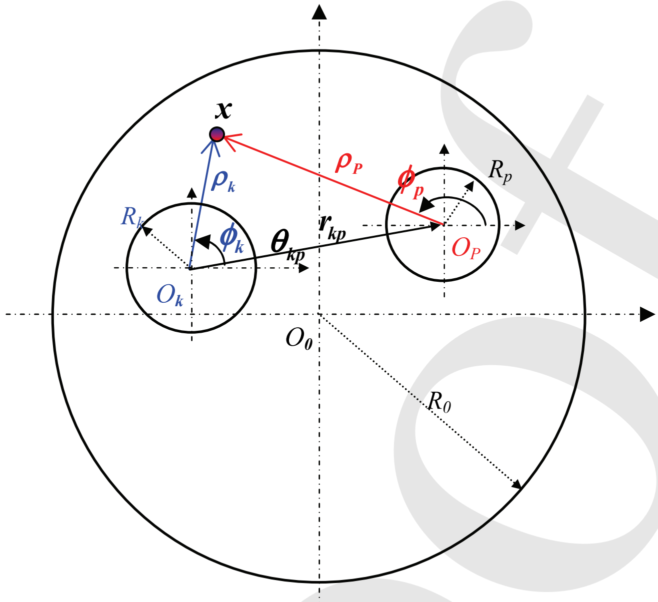

Figure 2: Notation of the Graf's addition theorem for Bessel functions

Furthermore, Eq. (16) can be rewritten as

$$
\begin{aligned}
& w(x;\rho_0,\phi_0) \\
& = \sum_{m=-\infty}^{\infty} e^{im\phi_0} \left\langle J_m(\lambda\rho_0)a_m^0 + I_m(\lambda\rho_0)b_m^0 \right. \\
& \qquad \left. + \sum_{k=1}^{H} \left[\sum_{n=-\infty}^{\infty} A_{mn}^k(\lambda\rho_0)a_n^k + \sum_{n=-\infty}^{\infty} B_{mn}^k(\lambda\rho_0)b_n^k \right] \right\rangle, \qquad (17)
\end{aligned}
$$

where

$$A_{mn}^k(\lambda\rho_0) = \mathrm{e}^{i(n-m)\theta_{k0}} J_{n-m}(\lambda r_{k0}) H_m^{(1)}(\lambda\rho_0), \qquad (18)$$

$$B_{mn}^k(\lambda\rho_0) = (-1)^{n-m} \mathrm{e}^{i(n-m)\theta_{k0}} I_{n-m}(\lambda r_{k0}) K_m(\lambda\rho_0). \qquad (19)$$

By differentiating Eq. (17) with respect toρ_0, the slope θ near the circular boundary

B_0 is given by

$$\theta(x;\rho_0,\phi_0) = \sum_{m=-\infty}^{\infty} e^{im\phi_0} \Big\langle \lambda J'_m(\lambda\rho_0)a_m^0 + \lambda I'_m(\lambda\rho_0)b_m^0 + \sum_{k=1}^{H}\Big[\sum_{n=-\infty}^{\infty} C_{mn}^k(\lambda\rho_0)a_n^k + \sum_{n=-\infty}^{\infty} D_{mn}^k(\lambda\rho_0)b_n^k\Big]\Big\rangle, \quad (20)$$

where $C_{mn}^k(k\rho_0)$ and $D_{mn}^k(k\rho_0)$ are obtained by differentiating $A_{mn}^k(k\rho_0)$ and $B_{mn}^k(k\rho_0)$ in Eqs. (18) and (19) with respective to ρ_0.

By substituting Eq. (11) into Eq. (9) and applying the addition theorem under the condition $\rho_p < r_{kp}$, the field of bending moment, $m(x)$, near the circular boundary B_p ($p = 1,\ldots, H$) can be expanded as follows:

$$m(x;\rho_p,\phi_p) = \sum_{m=-\infty}^{\infty} \mathrm{e}^{im\phi_p} \Big\langle E_m^p(\lambda\rho_p)a_m^p + F_m^p(\lambda\rho_p)b_m^p + \sum_{\substack{k=0\\ k\neq p}}^{H}\Big[\sum_{n=-\infty}^{\infty} E_{mn}^k(\lambda\rho_p)a_n^k + \sum_{n=-\infty}^{\infty} F_{mn}^k(\lambda\rho_p)b_n^k\Big]\Big\rangle, \quad (21)$$

where

$$E_m^p(\lambda\rho_p) = \alpha_m^J(\lambda\rho_p) + i\alpha_m^Y(\lambda\rho_p), \quad (22)$$

$$F_m^p(\lambda\rho_p) = \alpha_m^K(\lambda\rho_p), \quad (23)$$

$$E_{mn}^k(\lambda\rho_p) = \begin{cases} \mathrm{e}^{i(n-m)\theta_{kp}}\alpha_m^J(\lambda\rho_p)J_{n-m}(\lambda r_{kp}), & k=0 \\ \mathrm{e}^{i(n-m)\theta_{kp}}\alpha_m^J(\lambda\rho_p)H_{n-m}^{(1)}(\lambda r_{kp}), & k\neq 0,p \end{cases}, \quad (24)$$

$$F_{mn}^k(\lambda\rho_p) = \begin{cases} \mathrm{e}^{i(n-m)\theta_{kp}}\alpha_m^I(\lambda\rho_p)I_{n-m}(\lambda r_{kp}), & k=0 \\ (-1)^m\mathrm{e}^{i(n-m)\theta_{kp}}\alpha_m^I(\lambda\rho_p)K_{n-m}(\lambda r_{kp}), & k\neq 0,p \end{cases}, \quad (25)$$

in which the moment operator $\alpha_m^X(\lambda\rho)$ from Eq. (9) is defined as

$$\alpha_m^X(\lambda\rho) = D\left\{(1-\mu)\frac{X'_m(\lambda\rho)}{\rho} - \left[(1-\mu)\frac{m^2}{\rho^2} \mp \lambda^2\right]X_m(\lambda\rho)\right\}, \quad (26)$$

where the upper (lower) signs refer to $X= J, Y, (I, K)$, respectively. The differential equations of the Bessel function have been used to simplify $\alpha_m^X(\lambda\rho)$.

Similarly, the effective shear operator $\beta_m^X(\lambda\rho)$ derived from Eq. (10) can be expressed as shown below:

$$\beta_m^X(\lambda\rho) = D\left\{\left[m^2(1-\mu)\pm(\lambda\rho)^2\right]\frac{X_m'(\lambda\rho)}{\rho^2} - m^2(1-\mu)\frac{X_m(\lambda\rho)}{\rho^3}\right\}, \tag{27}$$

and the field of effective shear, $v(\boldsymbol{x})$, near the circular boundary B_p ($p = 1,\ldots, H$) can be given by

$$\begin{aligned} v(x;\rho_p,\phi_p) = \sum_{m=-\infty}^{\infty} \mathrm{e}^{im\phi_p}\Big\langle & G_m^p(\lambda\rho_p)a_m^p + H_m^p(\lambda\rho_p)b_m^p \\ & + \sum_{\substack{k=1\\k\neq p}}^{H}\left[\sum_{n=-\infty}^{\infty} G_{mn}^k(\lambda\rho_p)a_n^k + \sum_{n=-\infty}^{\infty} H_{mn}^k(\lambda\rho_p)b_n^k\right]\Big\rangle, \end{aligned} \tag{28}$$

where $G_m^p(\lambda\rho_p)$,$H_m^p(\lambda\rho_p)$,$G_{mn}^k(\lambda\rho_p)$and $H_{mn}^k(k\rho_p)$ are obtained by replacing $\alpha_m^X(\lambda\rho_p)$ in Eqs. (22)-(25) with $\beta_m^X(\lambda\rho_p)$.

For an outer clamped circular plate (u = θ = 0) containing multiple circular holes with the free edge (m= v = 0), applying the orthogonal property of $\{\mathrm{e}^{im\phi_P}\}$ to Eqs.(17), (20), (21) and (28), respectively, and setting ρ_p equal to R_p give

$$\begin{cases} J_m(\lambda R_0)a_m^0 + I_m(\lambda R_0)b_m^0 - \sum\limits_{k=1}^{H}\left[\sum\limits_{n=-\infty}^{\infty} A_{mn}^k(\lambda R_0)a_n^k + \sum\limits_{n=-\infty}^{\infty} B_{mn}^k(\lambda R_0)b_n^k\right] = 0 \\ \lambda J_m'(\lambda R_0)a_m^0 + \lambda I_m'(\lambda R_0)b_m^0 - \sum\limits_{k=1}^{H}\left[\sum\limits_{n=-\infty}^{\infty} C_{mn}^k(\lambda R_0)a_n^k + \sum\limits_{n=-\infty}^{\infty} D_{mn}^k(\lambda R_0)b_n^k\right] = 0 \\ E_m^p(\lambda R_p)a_m^p + F_m^p(\lambda R_p)b_m^p + \sum\limits_{\substack{k=0\\k\neq p}}^{H}\left[\sum\limits_{n=-\infty}^{\infty} E_{mn}^k(\lambda R_p)a_n^k + \sum\limits_{n=-\infty}^{\infty} F_{mn}^k(\lambda R_p)b_n^k\right] = 0 \\ G_m^p(\lambda R_p)a_m^p + H_m^p(\lambda R_p)b_m^p + \sum\limits_{\substack{k=0\\k\neq p}}^{H}\left[\sum\limits_{n=-\infty}^{\infty} G_{mn}^k(\lambda R_p)a_n^k + \sum\limits_{n=-\infty}^{\infty} H_{mn}^k(\lambda R_p)b_n^k\right] = 0 \end{cases}, \tag{29}$$

for m=0, ±1, ±2, ..., n=0, ±1, ±2, ..., and p= 1, ..., H. Eq. (29) is a coupled infinite system of simultaneous linear algebraic equations which is the analytical model for the free vibration of a clamped circular plate containing multiple holes with the free edge. In order to evaluate the numerical results in the following section, the infinite system of Eq. (29) is truncated to a $(H+1)(2M+1)$ finite system of equations, i.e. m=0, ± 1, ± 2, …, $\pm M$. According to the direct-searching scheme, the natural frequencies are determined as the minimum singular value of the truncated finite system by using the SVD technique. Once the eigenvectors (i.e. the coefficients a_m^k and b_m^k, k=0,…, H; m=0, ± 1, ± 2,…, $\pm M$) are found, the associated natural modes can be obtained by substituting them into the multipole representation for the transverse displacement of Eq.(11).

4 Numerical results and discussions

To demonstrate the validity of the proposed method, the FORTRAN code was implemented to determine natural frequencies and modes of a circular plate with multiple circular holes. The same problem was independently solved by using the FEM (the ABAQUS software) for comparison. In all cases, the inner boundary is subject to the free boundary condition. The thickness of plate is 0.002m and the Poisson's ratio μ=1/3. The general-purpose linear triangular elements of type S3 were employed to model the plate problem by using the ABAQUS software. Although the thickness of the plate is 0.002 m, these elements do not suffer from the transverse shear locking based on the theoretical manual of ABAQUS.

Case 1: A circular plate with an eccentric hole [Lee and Chen (2008a)]

A clamped circular plate containing an eccentric hole with a free edge as shown in Fig. 3 is considered. The lower seven natural frequency parameters versus the number of coefficients in Eq. (11), $N(2M+1)$, are shown in Fig. 4. It can be seen that the proposed solution converges fast by using only a few numbers of coefficients. Values of m and n in the mode (m,n) [Lee and Chen (2008a)] shown in Fig. 4 are numbers of diametrical nodal lines and circular nodal lines, respectively. For the mode (m, 0) in Fig. 4, two corresponding modes are clearly distinguished by the subscript. The subscript 1 denotes the straight diametrical nodal line, while the subscript 2 denotes the curved diametrical nodal line [Lee and Chen (2008a)]. It indicates that the required number of coefficients equals to that of diametrical nodal lines except to the mode with the subscript 2 due to the more complicated configuration. That is the reason why the higher mode (1, 1) can be roughly predicted by using only M=1 (or N=3). Figure 5 indicates the minimum singular value of Eq. (29) versus the frequency parameterλ when using thirteen numbers of coefficients (N=13). Since the direct-searching scheme is used, the drop location indicates the eigenvalue. No spurious eigenvalue is found by using the present method. The FEM was employed to solve the same problem and its model needs 164580 elements and 83023 nodes to obtain acceptable results for comparison. The lower six

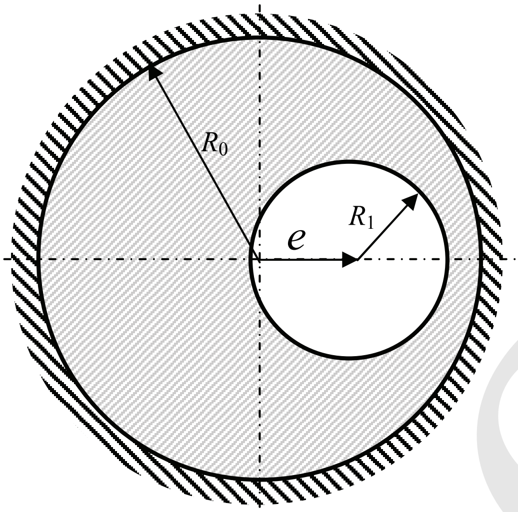

<u>*Case 1*:</u>

Geometric data:
R_0=1m
R_1=0.4m
e=0.5m
thickness=0.002m
Boundary condition:
Inner circle : free
Outer circle: clamped

Figure 3: A clamped circular plate containing an eccentric hole with a free edge

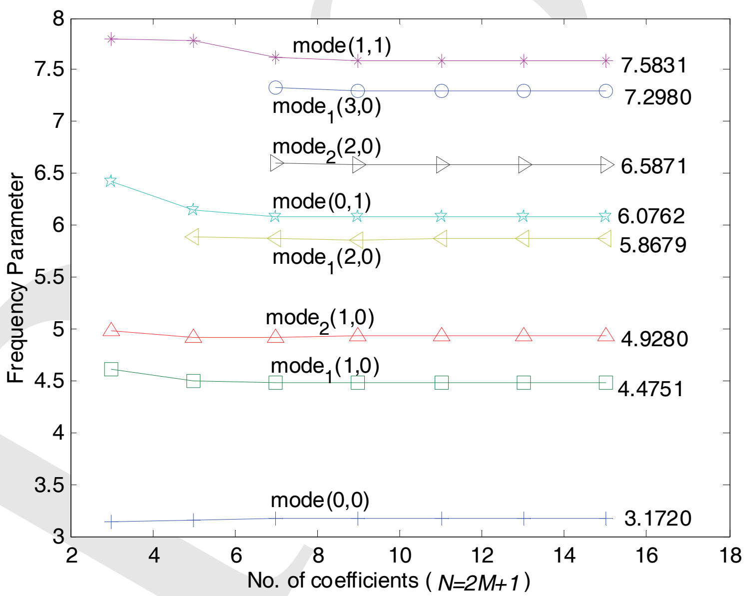

Figure 4: Natural frequency parameter versus the number of coefficients of the multipole representation for a clamped circular plate containing an eccentric hole with a free edge (R_0=1.0, R_1=0.4 and e/R_0=0.5)

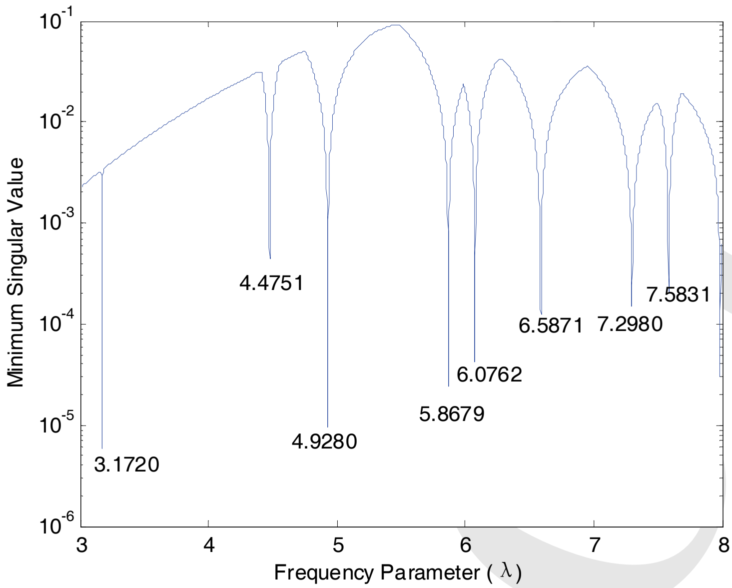

Figure 5: The minimum singular value versus the frequency parameter for a clamped circular plate containing an eccentric hole with a free edge (R_0=1.0, R_1=0.4 and e/R_0=0.5)

natural frequency parameters and modes by using the present method, the semi-analytical method [Lee, Chen and Lee (2007)] and the FEM are shown in Fig. 6. The results of the present method match well with those of FEM by using the ABAQUS software.

Case 2: A circular plate with two holes

To investigate the hole-hole interaction, a circular plate containing two identical holes with various ratio of L/a shown in Fig. 7 is studied, where a is the radius of circular holes and L is the central distance of two holes. The radii of the circular plate and the circular hole are 1 m and 0.1 m and the dimensionless distance of two holes L/a is chosen as 2.1, 2.5 and 4.0 in the numerical experiments. From the numerical results, the space of two holes has a minor effect on the lower natural frequency parameters. Figure 8 is the fundamental natural mode for the cases of L/a=2.1 and L/a=4.0. It can be seen that the zone of the maximum deformation, enclosed with the dashed line, for the case of L/a=2.1 is significantly less than that of L/a=4.0. It can account for the dynamic stress concentration in the case of L/a=2.1 [Lee and Chen (2008b)] because the distortion energy caused by the external loading concentrates in the smaller area.

Mode No.	1	2	3	4	5	6	7
Mode type	Mode(0,0)	$\text{Mode}_1(1,0)$	$\text{Mode}_2(1,0)$	$\text{Mode}_1(2,0)$	Mode(0,1)	$\text{Mode}_2(2,0)$	$\text{Mode}_1(3,0)$
Frequency parameter	3.1720	4.4751	4.9280	5.8679	6.0762	6.5871	7.2980
Present method	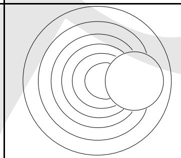	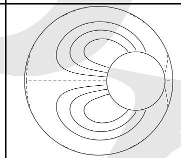	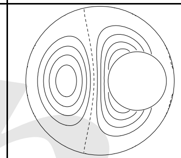	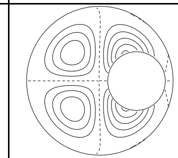	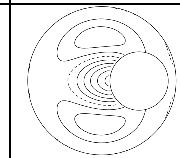	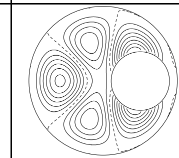	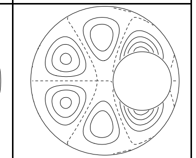
Frequency parameter	3.1721	4.4753	4.9281	5.8689	6.0762	6.5875	7.3031
Semi-analytical method [Lee and Chen (2008a)]	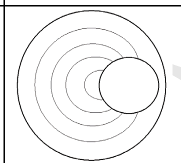	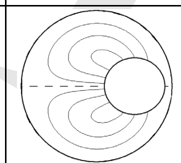	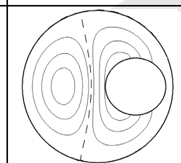	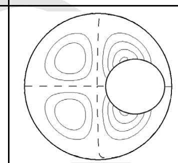	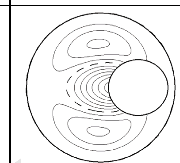	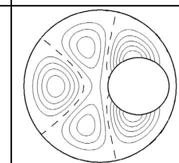	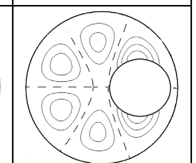
Frequency parameter	3.1724	4.4749	4.9278	5.8682	6.0757	6.5869	7.3020
ABAQUS	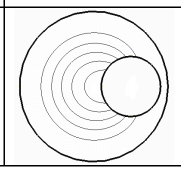	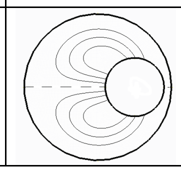	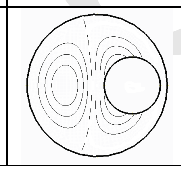	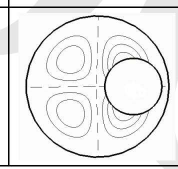	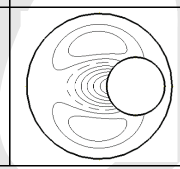	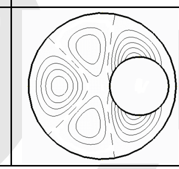	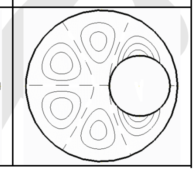

Figure 6: The lower seven frequency parameters, mode types and mode shapes for a clamped circular plate containing an eccentric hole with a free edge by using the present method, semi-analytical method and FEM (R_0=1.0, R_1=0.4 and e/R_0=0.5)

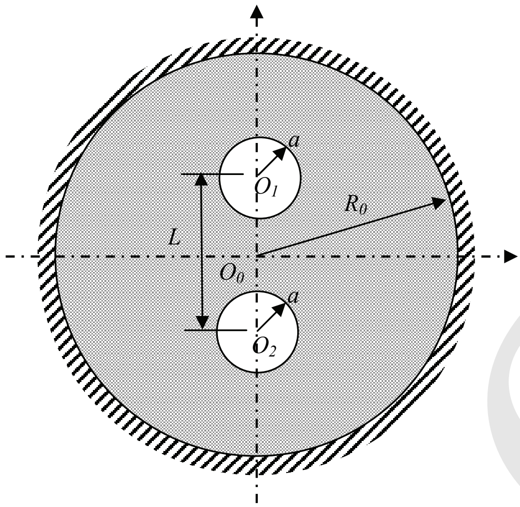

Case 2:

Geometric data:
R_0=1m
a=0.1m
thickness=0.002m
Boundary condition:
Inner circle : free
Outer circle: clamped

Figure 7: A clamped circular plate containing three holes with free edges

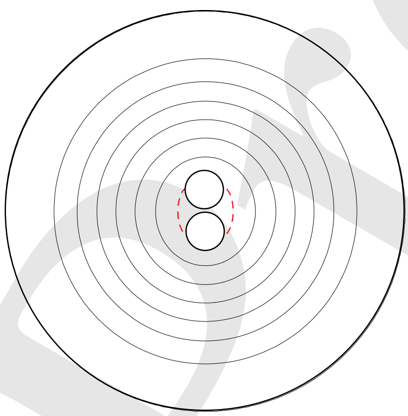

(a) Natural frequency parameter=3.1720

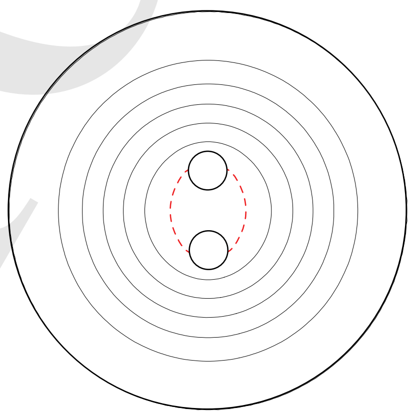

(b) Natural frequency parameter=3.1800

Figure 8: Natural frequency parameter versus the number of coefficients of the multipole representation for a clamped circular plate containing three holes with free edges

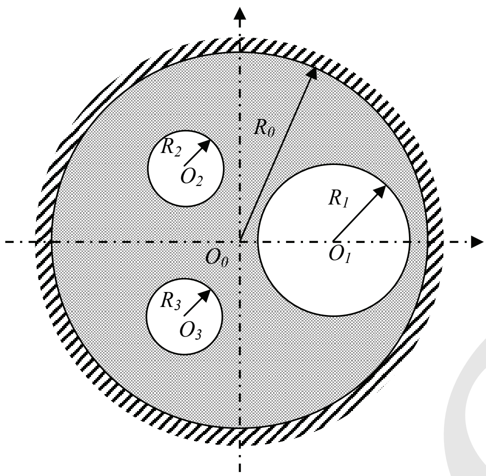

<u>*Case 3*:</u>
Geometric data:
R_0=1m
R_1=0.4m
R_2=0.2m
R_3=0.2m
O_0=(0.0,0.0)
O_1=(0.5,0.0)
O_2=(−0.3,0.4)
O_3=(−0.3,−0.4)
thickness=0.002m
Boundary condition:
Inner circles: free
Outer circle: clamped,

Figure 9: The minimum singular value versus the frequency parameter for a clamped circular plate containing three holes with free edges

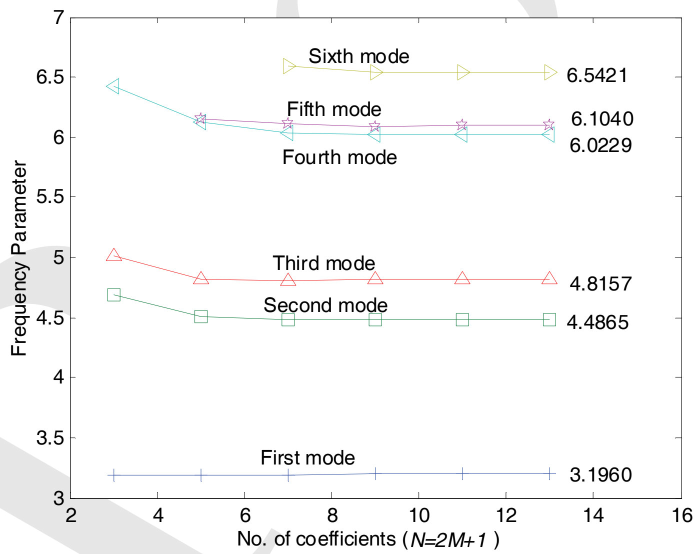

Figure 10: The lower six natural frequency parameters and mode shapes for a clamped circular plate containing three holes with free edge by using the present method, semi-analytical method and FEM

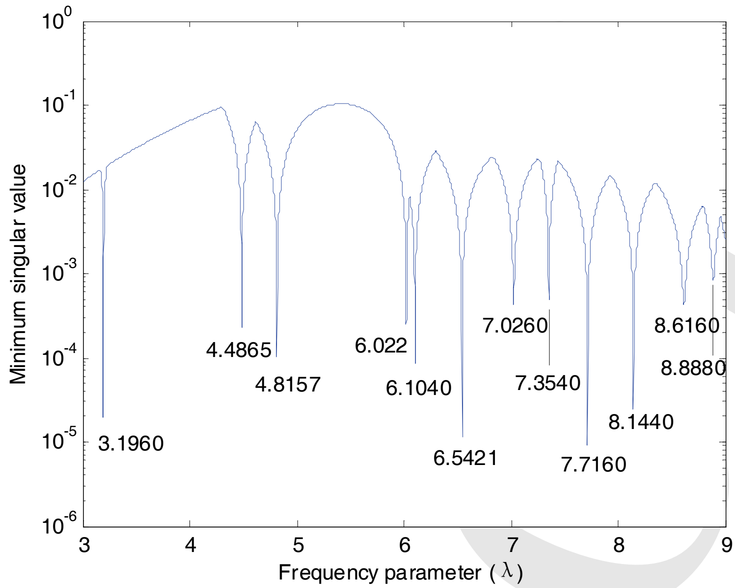

Figure 11: The minimum singular value versus the frequency parameter for a clamped circular plate containing three holes with free edges

182 *Case 3: A circular plate with three holes* [Lee and Chen (2008a)]

183 In order to demonstrate the generality of the present method, a circular plate with three holes is considered as shown in Fig 9. The lower six natural frequency parameters versus the number of coefficients in Eq. (11) are shown in Fig. 10. When the number of holes increases, the fast convergence rate can still be observed. The fourth mode shows a lower convergence rate due to the complex geometrical configuration. Figure 11 indicates the minimum singular value of Eq. (29) versus the frequency parameter λ when using thirteen terms of Fourier series (N=13). There is no spurious eigenvalue [Lee and Chen (2008a)] since zero divided by zero is analytically determined in the present method. To achieve the satisfactory solution for comparison, the model of FEM needs 308960 elements. The lower six natural frequency parameters and modes by using the present method, the semi-analytical method [Lee and Chen (2008a)] and the FEM are shown in Fig. 12. Good agreement between the results of the present method and those of ABAQUS is observed.

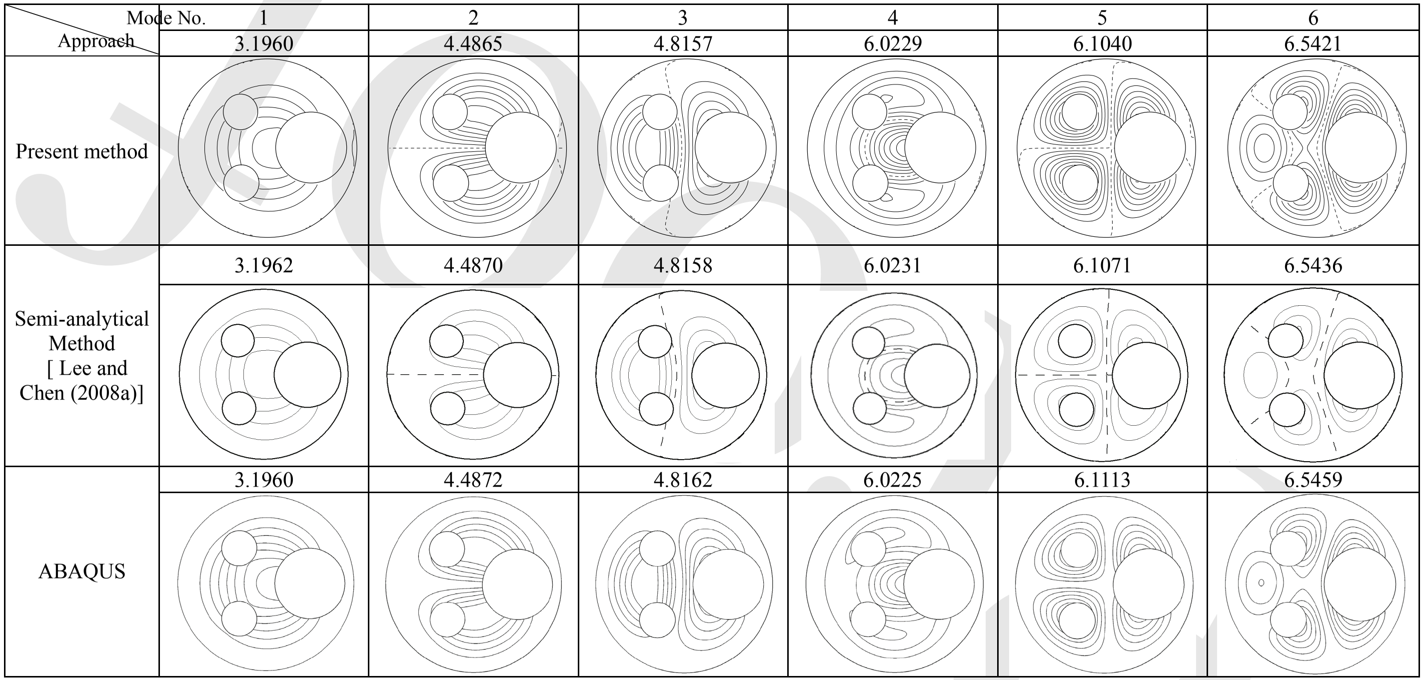

Figure 12: The lower six natural frequency parameters and mode shapes for a clamped circular plate containing three holes with free edges by using the present method, semi-analytical method and FEM

5 Concluding remarks

By using the addition theorem, the multipole Trefftz method has successively derived an analytical model for a circular plate containing multiple circular holes. According to the specified boundary conditions, a coupled infinite system of simultaneous linear algebraic equations was derived without any approximation. By using the direct-searching method, natural frequencies and natural modes of the stated problem were given in the truncated finite system. The proposed results match well with those provided by the FEM with more fine mesh to obtain acceptable data for comparison. No spurious eigenvalue occurs in the present formulation. Moreover, the proposed eigensolutions have attempted explanations for the dynamic stress concentration when two holes are close to each other. Numerical results show good accuracy and fast rate of convergence thanks to the analytical approach.

References

Alves, C. J. S.; Antunes, P. R. S. (2005): The Method of Fundamental Solutions applied to the calculation of eigenfrequencies and eigenmodes of 2D simply connected shapes. *CMC: Computers, Materials & Continua*, vol. 2, pp. 251–266.

Chen, C. W.; Fan, C. M.; Young, D. L.; Murugesan, K.; Tsai, C. C. (2005): Eigenanalysis for Membranes with Stringers Using the Methods of Fundamental Solutions and Domain Decomposition. *CMES: Computer Modeling in Engineering & Sciences*, vol. 8, pp. 29–44.

Cheng, L.; Li, Y. Y.; Yam, L. H. (2003): Vibration analysis of annular-like plates. *Journal of Sound and Vibration,* vol. 262, pp. 1153-1170.

Kamiya, N.; Kita, E. (1995): Trefftz method: an overview. *Advances in Engineering Software*, vol. 24, pp. 3-12.

Khurasia, H. B.; Rawtani, S. (1978): Vibration analysis of circular plates with eccentric hole. *ASME Journal of Applied Mechanics*, vol. 45, pp. 215-217.

Kitahara, M. (1985): Boundary Integral Equation Methods in Eigenvalue Problems of Elastodynamics and Thin Plates. Elsevier: Amsterdam.

Laura, P. A. A.; Masia, U.; Avalos, D. R. (2006): Small amplitude, transverse vibrations of circular plates elastically restrained against rotation with an eccentric circular perforation with a free edge. *Journal of Sound and Vibration,* vol. 292, pp. 1004-1010.

Lee, W. M.; Chen, J. T.; Lee, Y. T. (2007): Free vibration analysis of circular plates with multiple circular holes using indirect BIEMs. *Journal of Sound and Vibration,* vol. 304, pp.811-830.

Lee, W. M.; Chen, J. T. (2008a): Null-field integral equation approach for free vibration analysis of circular plates with multiple circular holes. *Computational Mechanics*, vol. 42, pp.733–747.

Lee, W. M.; Chen, J. T. (2008b): Scattering of flexural wave in thin plate with multiple holes by using the null-field integral equation approach. *CMES: Computer Modeling in Engineering & Science*, vol. 37, No. 3, pp. 243-273.

Leissa, A. W.; Narita, Y. (1980): Natural frequencies of simply supported circular plates. *Journal of Sound and Vibration*, vol. 70, pp. 221-229.

Linton, C. M.; Evans, D. V. (1990): The interaction of waves with arrays of vertical circular cylinders. *Journal Fluid Mechanics*, vol. 215, pp. 549-569.

Martin, P. A. (2006): Multiple scattering interaction of time-harmonic wave with N obstacles. Cambridge University Press, UK.

Reutskiy, P. Yu. (2005): The method of fundamental solutions for eigenproblems with Laplace and biharmonic operators. *CMC: Computers, Materials & Continua*, vol. 2, No. 3, pp. 177-188.

Reutskiy, P. Yu. (2006): The Method of External Sources (MES) for Eigenvalue Problems with Helmholtz Equation. *CMES: Computer Modeling in Engineering & Sciences*, vol. 12, No. 1. pp. 27-39.

Reutskiy, P. Yu. (2007): The method of fundamental solutions for problems of free vibrations of plates. *Engineering Analysis with Boundary Elements*, vol. 31, pp. 10-21.

Tseng, J. G; Wickert, J. A. (1994): Vibration of an eccentrically clamped annular plate. *ASME Journal of Applied Mechanics*, vol. 116, pp. 155-160.

Trefftz, E. (1926): Ein Gegensttick zum Ritz' schen Verfahren. Proc. Second Int. Cong. Applied. Mechanics., Zurich, pp. 131-137.

Vega, D. A.; Vera, S. A.; Sanchez, M. D.; Laura, P. A. A. (1998): Transverse vibrations of circular, annular plates with a free inner boundary. *Journal of Acoustic Society. America*, vol. 103, pp. 1225-1226.

Vera, S. A.; Laura, P. A. A.; Vega, D. A. (1999): Transverse vibrations of a free-free circular annular plate. *Journal of Sound and Vibration*, vol. 224 No. 2, pp. 379-383.

Vera, S. A.; Sanchez, M. D.; Laura, P. A. A.; Vega, D. A. (1998): Transverse vibrations of circular, annular plates with several combinations of boundary conditions. *Journal of Sound and Vibration*, vol. 213, No. 4, pp.757-762.

Vogel, S. M; Skinner, D. W. (1965): Natural frequencies of transversely vibrating uniform annular plates, *ASME Journal of Applied Mechanics*, vol. 32, pp. 926-931.

Watson, G. N. (1995): A treatise on the theory of Bessel Functions, second edition. Cambridge: Cambridge Library edition.

Záviška, F. (1913): Uber die Beugung elektromagnetischer Wellen an parallelen, unendlich langen Kreiszylindern. *Annalen der Physik*, 4 Folge, vol. 40, pp. 1023-1056.